

See discussions, stats, and author profiles for this publication at: <https://www.researchgate.net/publication/8557434>

# Hydrogen bond driven chemical reactions: Beckmann rearrangement of cyclohexanone oxime into $\epsilon$ -Caprolactam in supercritical water

ARTICLE *in* JOURNAL OF THE AMERICAN CHEMICAL SOCIETY · JUNE 2004

Impact Factor: 12.11 · DOI: 10.1021/ja049363f · Source: PubMed

---

CITATIONS

99

---

READS

379

5 AUTHORS, INCLUDING:



**Mauro Boero**

Institut de Physique et Chimie des Matériaux ...

187 PUBLICATIONS 3,480 CITATIONS

SEE PROFILE



**K. Terakura**

National Institute of Advanced Industrial Sci...

374 PUBLICATIONS 13,209 CITATIONS

SEE PROFILE

## Hydrogen Bond Driven Chemical Reactions: Beckmann Rearrangement of Cyclohexanone Oxime into $\epsilon$ -Caprolactam in Supercritical Water

Mauro Boero,<sup>\*,†</sup> Tamio Ikeshoji, Chee Chin Liew,<sup>‡,||</sup> Kiyoyuki Terakura,<sup>‡,⊥</sup> and Michele Parrinello<sup>§</sup>

*Contribution from the Institute of Physics, University of Tsukuba, 1-1-1 Tennodai, Tsukuba, Ibaraki 305-8571, Japan, Research Institute for Computational Sciences, National Institute of Advanced Industrial Science and Technology, 1-1-1 Umezono, Tsukuba, Ibaraki 305-8568, Japan, Computational Science, Department of Chemistry and Applied Biosciences - ETH Zurich, USI Campus, via Giuseppe Buffi 13, CH-6900 Lugano, Switzerland, and Division of Frontier Research, Creative Research Initiative "Sousei", Hokkaido University, Kita 21, Nishi 10, Kita-ku, Sapporo 001-0021, Japan*

Received February 4, 2004; E-mail: boero@rccp.tsukuba.ac.jp

**Abstract:** Recent experiments have shown that supercritical water (SCW) has the ability to accelerate and make selective synthetic organic reactions, thus replacing the common but environmentally harmful acid and basic catalysts. In an attempt to understand the intimate mechanism behind this observation, we analyze, via first-principles molecular dynamics, the Beckmann rearrangement of cyclohexanone oxime into  $\epsilon$ -caprolactam in supercritical water, for which accurate experimental evidence has been reported. Differences in the wetting of the hydrophilic parts of the solute, enhanced by SCW, and the disrupted hydrogen bond network are shown to be crucial in triggering the reaction and in making it selective. Furthermore, the enhanced concentrations of  $H^+$  in SCW play an important role in starting the reaction.

### 1. Introduction

Particular attention has been paid in recent years to the environmental impact of industrial processes, and this has promoted considerable effort in so-called "green chemistry". In the search for environmentally harmless chemical processes, water above its critical point ( $T_c = 647$  K,  $P_c = 22$  MPa,  $\rho_c = 0.32$  g/cm<sup>3</sup>) plays a key role as a tool for the disposal of hazardous waste,<sup>1–3</sup> for geochemical reactions,<sup>4</sup> and, more recently, as a promoter of synthesis reactions.<sup>5–10</sup> The peculiarity of water, with respect to other polar solvents, stems from its unique hydrogen bond (H-bond) properties, known to be

responsible for the very rich phase diagram of H<sub>2</sub>O and for phenomena like proton wire transport mechanisms.<sup>11</sup> It can then be inferred that chemical reactions occurring in water could be tuned, provided that the H-bond network can be controlled. Indeed, experiments have shown that synthetic organic reactions, which generally require a strong acid to occur, can proceed in water without any catalyst when the fluid is brought above the critical point.<sup>7–10</sup> This is the case in the Beckmann rearrangement<sup>12</sup> of cyclohexanone oxime into  $\epsilon$ -caprolactam, important for its own sake as a textbook example of proton-triggered process, and because of its industrial use in the production of nylon synthetic fibers.<sup>8–14</sup> The reaction scheme is shown in the upper panels of Figure 1A: a proton, generally provided by strong acid catalysts, promotes the reaction leading to the formation of  $\epsilon$ -caprolactam. However, an alternative pathway is possible, shown in the lower panels: the proton attacks the nitrogen atom, inducing the formation of cyclohexanone and, upon hydrolysis, hydroxylamine NH<sub>2</sub>OH<sup>7</sup> (lower right panel). The latter is a typical byproduct of low commercial value, generated in acid-catalyzed reactions and found also in reactions occurring in superheated water.<sup>7,8</sup> On the other hand, it has been shown<sup>6–8</sup> that supercritical water (SCW) is able to promote selectively the "right" reaction. SCW is thus appealing not only

<sup>†</sup> University of Tsukuba.

<sup>‡</sup> National Institute of Advanced Industrial Science and Technology.

<sup>§</sup> Department of Chemistry and Applied Biosciences - ETH Zurich, USI Campus.

<sup>⊥</sup> Hokkaido University.

<sup>||</sup> Present address: BASF AG, Polymer Research Division, D-67056 Ludwigshafen, Germany.

- (1) *Emerging Technologies for Hazardous Waste Management III*; Tedder, D. W., Pohland, F. G., Eds.; ACS Symposium Series 518; American Chemical Society: Washington DC, 1993.
- (2) Lee, D. S.; Gloyne, E. F. *J. Supercrit. Fluids* **1990**, *3*, 249.
- (3) Yang, H. H.; Eckert, C. A. *Ind. Eng. Chem. Res.* **1988**, *27*, 2009.
- (4) Siskin, M.; Katritzky, A. R. *Science* **1991**, *254*, 231.
- (5) Bröll, D.; Kaul, C.; Krämer, A.; Krammer, P.; Richter, T.; Jung, M.; Vogel, H.; Zehner, P. *Angew. Chem., Int. Ed.* **1999**, *38*, 2999.
- (6) Ikushima, Y.; Hatake, K.; Sato, O.; Yokoyama, T.; Arai, M. *Angew. Chem., Int. Ed.* **1999**, *38*, 2910.
- (7) Sato, O.; Ikushima, Y.; Yokoyama, T. *J. Org. Chem.* **1998**, *63*, 9100.
- (8) Ikushima, Y.; Hatake, K.; Sato, O.; Yokoyama, T.; Arai, M. *J. Am. Chem. Soc.* **2000**, *122*, 1908.
- (9) Zhang, R.; Zhao, F. Y.; Sato, M.; Ikushima, Y. *Chem. Commun.* **2003**, *13*, 1548.
- (10) Ikushima, Y.; Sato, O.; Sato, M.; Hatake, K.; Arai, M. *Chem. Eng. Sci.* **2003**, *58*, 935.

(11) Pomès, R.; Roux, B. *J. Phys. Chem.* **1996**, *100*, 2519.

(12) Donaruma, L. J.; Heldt, W. Z. In *Organic Reactions*; The Beckmann Rearrangement, Vol. 11; Wiley & Sons: New York, 1960.

(13) Dahlhoff, G.; Niederer, J. P. M.; Hölderich, W. F. *Catal. Rev.* **2001**, *43*, 381.

(14) Yamaguchi, Y.; Yasutake, N.; Nagaoka, M. *J. Mol. Struct. (THEOCHEM)* **2003**, *639*, 137 (15) Car, R.; Parrinello, M. *Phys. Rev. Lett.* **1985**, *55*, 2471.

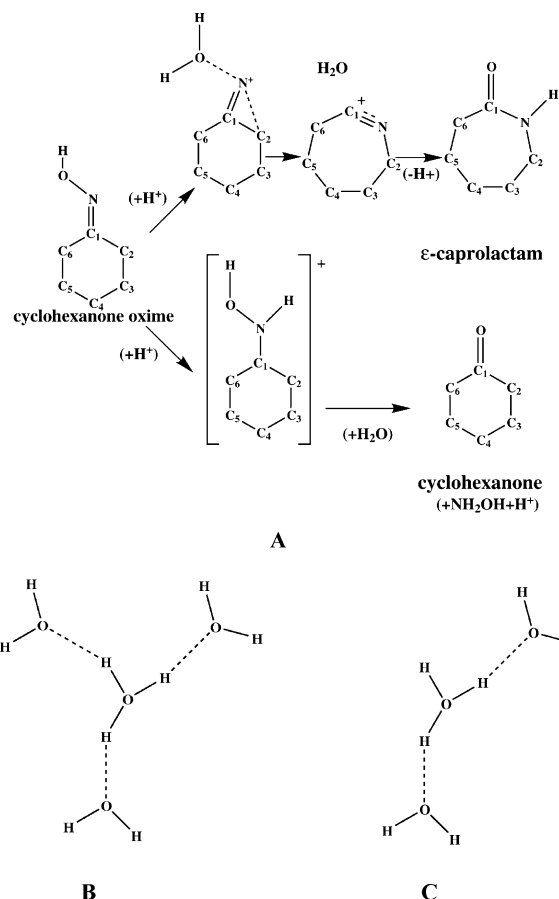


**Figure 1.** (A) Reaction path leading to the formation of  $\epsilon$ -caprolactam from cyclohexanone oxime (upper panels) and the competing alternative pathway (lower panels). The labeling of the atoms is the one used throughout the text. Panels are intended only as an example of a pathway and not as the actual configurations of the transition states. (B) Eigen  $\text{H}_9\text{O}_4^+$  complex in normal liquid water. (C) Defective Eigen  $\text{H}_7\text{O}_3^+$  complex in SCW.

because it is harmless in comparison with the industrially used acids but also because of its intrinsically selective character. Nonetheless, despite the high quality of the experimental efforts, the details of the reaction, as well as the role played by water, have thus far escaped accurate determination. In an attempt to shed some light on the general reaction mechanism, we performed first-principles molecular dynamics simulations within the Car–Parrinello (CPMD) scheme<sup>15,16</sup> using three systems consisting of a single cyclohexanone oxime molecule surrounded by 60 water molecules at the thermodynamic conditions ( $T = 673 \text{ K}$ ,  $\rho = 0.66 \text{ g/cm}^3$ ), ( $T = 300 \text{ K}$ ,  $\rho = 1.00 \text{ g/cm}^3$ ), and ( $T = 673 \text{ K}$ ,  $\rho = 1.00 \text{ g/cm}^3$ ), to inspect the effects of both density and temperature.

## 2. Computational Details

Car–Parrinello simulations<sup>15,16</sup> including the generalized gradient approximation after Becke–Lee–Yang–Parr<sup>17,18</sup> for the exchange–correlation functional were performed on three systems at the three thermodynamic conditions ( $T = 673 \text{ K}$ ,  $\rho = 0.66 \text{ g/cm}^3$ ), ( $T = 300 \text{ K}$ ,  $\rho = 1.00 \text{ g/cm}^3$ ), and ( $T = 673 \text{ K}$ ,  $\rho = 1.00 \text{ g/cm}^3$ ). Norm-conserving pseudopotentials<sup>19</sup> accounted for the core–valence interaction, and

valence wave functions were expanded in a plane wave basis set with a cutoff energy of 70 Ry. The temperature control was ensured by a Nosé–Hoover thermostat.<sup>20,21</sup>

We first equilibrated for about 6 ps three (NVT) ensembles consisting of 64 water molecules in cubic supercells with periodic boundary conditions. Then we cleaved the required space, corresponding to four water monomers, to allocate the cyclohexanone oxime and reequilibrated the systems for about 5 ps. Auxiliary simulations using the 64-water-molecule systems at the three different thermodynamic conditions plus one excess proton were performed for about 18 ps to investigate the  $\text{H}^+$  diffusion mechanism. The accuracy of our computational approach in describing the properties of SCW has been assessed in previous works<sup>22–25</sup> and has been shown to be capable of reproducing the known experimental results.<sup>26–28</sup>

Whenever an activation barrier has to be overcome, we sampled the reaction path via both Blue Moon ensemble theory<sup>29</sup> and the newly introduced metadynamics approach<sup>30,31</sup> by adding to the Car–Parrinello Lagrangian  $L^{\text{CP}}$  the slow degrees of freedom represented by collective variables  $s_\alpha(t)$  plus a history-dependent Gaussian potential  $V(s_\alpha, t)$

$$L = L^{\text{CP}} + \sum_{\alpha} \frac{1}{2} M_{\alpha} \dot{s}_{\alpha}^2(\vec{R}_I) - \sum_{\alpha} \frac{1}{2} k_{\alpha} [s_{\alpha}(\vec{R}_I) - s_{\alpha}^0]^2 + V(s_{\alpha}, t) \quad (1)$$

as described in ref 30. Details regarding the particular collective variables selected and the values of the parameters adopted will be given in the following section for each of the cases discussed.

Mulliken charges are computed by a standard projection of the Kohn–Sham states onto atomic orbitals.<sup>32</sup>

## 3. Results and Discussion

**3.1. Solvation Properties of O and N.** Free CPMD simulations performed for about 6 ps on the three solutions have shown that the disrupted H-bond network of SCW alters the solvation of both the oxygen (O) and the nitrogen (N) atoms of the solute molecule, with respect to ordinary liquid water. In Figure 2 theoretical partial pair correlation functions of the O and N atoms of the cyclohexanone oxime with the oxygen (Ow) and hydrogen (Hw) atoms of the surrounding water molecules are reported for the three thermodynamic conditions examined. As can be seen (Figure 2A), while  $g_{\text{O–Ow}}(r)$  still shows a peak at  $\sim 3\text{--}3.5 \text{ \AA}$ —typical of H-bond structures<sup>33,34</sup>—also at supercritical conditions (upper panel, curve (c)), the corresponding pair correlation function of nitrogen  $g_{\text{N–Ow}}(r)$  (lower panel, curve (c)) becomes practically structureless: a depletion hole forms around N. Analogously, the pair correlation functions  $g_{\text{O–Hw}}(r)$  and  $g_{\text{N–Hw}}(r)$  (Figure 2B, curves (c) in both upper and lower panels) show that the peak at  $\sim 1.8 \text{ \AA}$  due to the H-bond with

- (15) Car, R.; Parrinello, M. *Phys. Rev. Lett.* **1985**, *55*, 2471.
- (16) Hutter, J. et al. CPMD code; MPI für Festkörperforschung und IBM Zurich Research Laboratory, 1990–2003.
- (17) Becke, A. D. *Phys. Rev. A* **1988**, *38*, 3098.
- (18) Lee, C.; Yang, W.; Parr, R. G. *Phys. Rev. B* **1988**, *37*, 785.
- (19) Troullier, N.; Martins, J. L. *Phys. Rev. B* **1991**, *43*, 1993.

- (20) Nosé, S. *Mol. Phys.* **1984**, *52*, 255.
- (21) Hoover, W. G. *Phys. Rev. B* **1985**, *31*, 1695.
- (22) Boero, M.; Terakura, K.; Ikeshoji, T.; Liew, C. C.; Parrinello, M. *Phys. Rev. Lett.* **2000**, *85*, 3245.
- (23) Boero, M.; Terakura, K.; Ikeshoji, T.; Liew, C. C.; Parrinello, M. *J. Chem. Phys.* **2001**, *115*, 2219.
- (24) Boero, M.; Parrinello, M.; Terakura, K.; Ikeshoji, T.; Liew, C. C. *Phys. Rev. Lett.* **2003**, *90*, 226403.
- (25) Ikushima, Y.; Sato, M.; Hatakeyama, K.; Ikeshoji, T.; Boero, M. *Int. J. Chem. Reactor Eng.* **2004**, In press.
- (26) Botti, A.; Bruni, F.; Ricci, M. A.; Soper, A. K. *J. Chem. Phys.* **1988**, *109*, 3180.
- (27) Tassaing, T.; Bellissent-Funel M.-C.; Guillot, B.; Guissani, Y. *Europhys. Lett.* **1998**, *42*, 265.
- (28) Lamb, W. J.; Hoffman, G. A.; Jonas, J. *J. Chem. Phys.* **1980**, *74*, 6875.
- (29) Sprick, M.; Ciccotti, G. *J. Chem. Phys.* **1998**, *109*, 7737.
- (30) Iannuzzi, M.; Laio, A.; Parrinello, M. *Phys. Rev. Lett.* **2003**, *90*, 238302.
- (31) Laio, A.; Parrinello, M. *Proc. Natl. Acad. Sci. U.S.A.* **2002**, *99*, 12562.
- (32) Segall, M. D.; Shah, R.; Pickard C. J.; Payne, M. C. *Phys. Rev. B* **1996**, *54*, 16317.
- (33) Bergman, D. L. *Chem. Phys.* **2000**, *253*, 267.
- (34) Baranyai, P. C.; Chialvo, A. A.; Cummings, P. T. *Mol. Simul.* **2003**, *29*, 13.

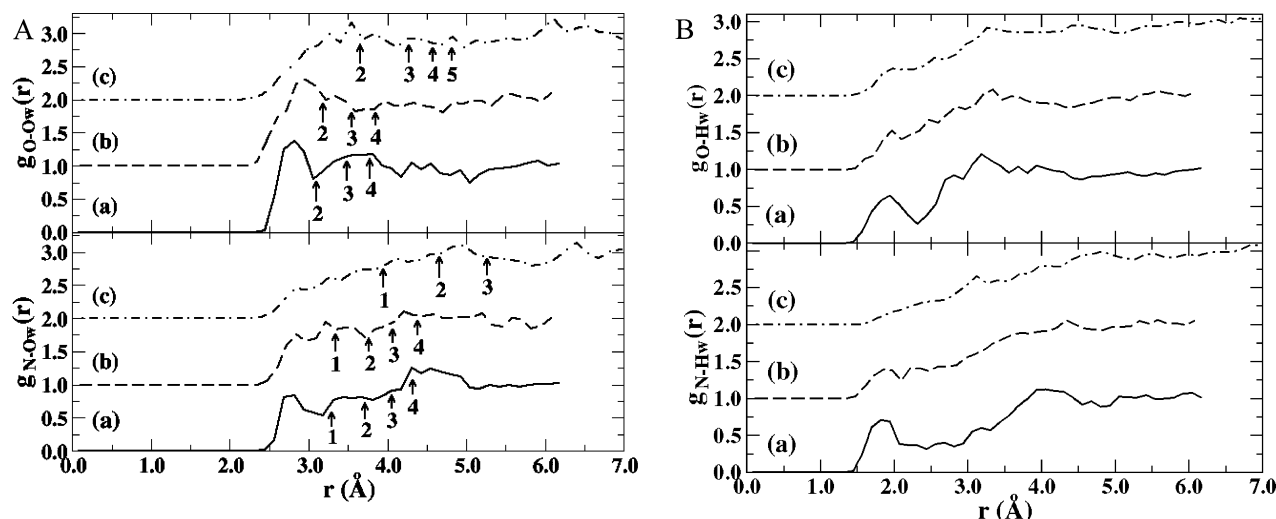


**Figure 2.** Theoretical partial pair correlation functions  $g_{\text{O-Ow}}(r)$  and  $g_{\text{N-Ow}}(r)$  (A) and  $g_{\text{O-Hw}}(r)$  and  $g_{\text{N-Hw}}(r)$  (B) at the thermodynamic conditions  $\rho = 1.0$  g/cm<sup>3</sup>,  $T = 300$  K (a),  $\rho = 1.0$  g/cm<sup>3</sup>,  $T = 673$  K (b) and  $\rho = 0.66$  g/cm<sup>3</sup>,  $T = 673$  K (c). The labels (a), (b), and (c) reported above the three curves in each panel refer to these three thermodynamic states, respectively. In panel (A) the numbers below the arrows indicate the integrated coordination numbers. In both panels, (b) curves have been shifted by +1 along the y-axis and (c) curves by +2 for the sake of clarity.

the closest Hw still survives in SCW as a shoulder in the case of the O atom of the solute, while the depletion around N is underscored by the structureless slope of  $g_{\text{N-Hw}}(r)$ . More evidently, the coordination numbers reported in Figure 2A show that in SCW at a distance of  $\sim 3.56$  Å two H<sub>2</sub>O molecules are H-bonded to the O of the solute, which is *wet* also at supercritical conditions, while N is *dry*, since its coordination number integrates only to 1 at a rather large distance ( $\sim 3.95$  Å). This is due to two factors. On one hand the O and N sites of the cyclohexanone oxime are not equally solvated even at ordinary liquid conditions. The N atom of the solute is partially shielded by both the OH group and the hydrocarbon ring and can generally form only one H-bond in the ordinary liquid phase<sup>35</sup> (Figures 2 and 3B). Thus, when the density lowers and, due to the high  $T$ , the entropic contribution increases, the difference in the solvation of O and N is amplified (Figure 3A). Furthermore, the O $\cdots$ H hydrogen bond (Experiment: 2.6 kcal/mol;<sup>36</sup> present calculation: 2.3 kcal/mol) turns out to be tighter<sup>35</sup> than the N $\cdots$ H one by about 1 kcal/mol, according to our calculations. As a result, N becomes *dry* in SCW while O is still *wet*. We note (Figure 2, curves (b) in all the panels) that raising the temperature without changing the density of the fluid does not dramatically alter the wetting of the hydrophilic parts of the solute with respect to the ordinary liquid water (Figure 2, curves (a) in all the panels). Instead, a reduction in the density deeply affects the distribution of H<sub>2</sub>O molecules around the cyclohexanone oxime and, in this respect, is an essential *general ingredient* in tuning the reaction.

**3.2. First Step: The Proton Attack. 3.2.1. Supercritical Water.** Since this is an acid-catalyzed process, protons are deemed essential to promote the reaction. The concentration of H<sup>+</sup> (and OH<sup>−</sup>) can be enhanced in SCW either because of an increase of the  $K_w$  due to the extreme thermodynamic conditions<sup>8,37</sup> or because protons are supplied by an external source.<sup>38</sup> We reproduced these conditions by introducing an excess proton

in the simulation cell. The H<sup>+</sup> can be transferred from molecule to molecule via a proton wire mechanism<sup>11</sup> only as long as a H-bond network exists. This is not always the case in SCW, since the density is lower than the ordinary liquid. However, when possible, the migration of H<sup>+</sup> occurs according to the Grothuss structural diffusion pathway,<sup>39</sup> via an exchange between an O–H  $\sigma$ -bond and a H-bond. Due to the rapid thermal motion and to the fact that the O site of the solute is *wet*, an unconstrained CPMD simulation has shown that in a time of  $\sim 1$  ps the proton can approach the cyclohexanone oxime on the *good* active site. As a result, the H<sup>+</sup> attacks the oxygen of the N–O–H group of the solute molecule (Figure 3C), and the reaction  $\text{H}^+ + \text{OH-R} \rightarrow \text{H}_2\text{O} + \text{R}^+$  occurs (Figure 3D and E), leading to the formation of a new water molecule and leaving behind the six-membered ring structure carrying the *dry* N<sup>+</sup> atom (Figure 3E). It can be observed that the fact that the N atom has a positive charge partially hinders the formation of N $\cdots$ H<sub>2</sub>O H-bonds, despite the fact that N is now unshielded. By analyzing the trajectories of the auxiliary simulations (see Computational Details section), we found that the excess proton diffuses from one water molecule (OH<sub>3</sub><sup>+</sup>) to the adjacent H-bonded one in a time  $\tau_{\text{SCW}} = 0.088 \pm 0.036$  ps in the connected part of the H-bond network. Since the supercritical state is characterized by density fluctuations, the H<sup>+</sup> diffusion process occurs on two scales: inside the connected part of the H-bond network (*sub-network*) and among different *sub-networks* that join as a consequence of the density fluctuations. Inside a *sub-network*, the excess proton spends some time in a Zundel H<sub>5</sub>O<sub>2</sub><sup>+</sup> configuration,<sup>40</sup> shared by two adjacent H<sub>2</sub>O molecules and then stabilizes for a short time ( $\tau_{\text{SCW}}$ ) as an OH<sub>3</sub><sup>+</sup>. However, the reduced density and the disrupted H-bond network make its stabilization as Eigen H<sub>9</sub>O<sub>4</sub><sup>+</sup> complex (Figure 1B) a less frequent event, and the fast density fluctuations, due to the high entropic contribution, help the proton to switch quickly

(35) Ishida, M.; Suzuki, T.; Ichihashi, H.; Shiga, A. *Catal. Today* **2003**, *87*, 187.

(36) Walrafen, G. E.; Fisher, M. R.; Hokmabadi, M. S.; Yang, W. H. *J. Chem. Phys.* **1986**, *85*, 6970.

(37) Macdonald, D. D.; Song, H.; Makela, K.; Emerson, R.; Ben-Haim, M. J. *J. Solution Chem.* **1992**, *21*, 849.

(38) In recent experiments, excess protons are also provided by low concentrations ( $\sim 10^{-4}$  M) of HCl and H<sub>2</sub>SO<sub>4</sub>. See, e.g.: Ikushima, Y.; Hatakeda, K.; Sato, M.; Sato, O.; Arai, M. *Chem. Comm.* **2002**, *19*, 2208.

(39) de Grothuss, C. J. T. *Ann. Chim.* **1806**, *LVIII*, 54.

(40) Marx, D.; Tuckerman, M. E.; Hutter, J.; Parrinello, M. *Nature* **1999**, *397*, 601.

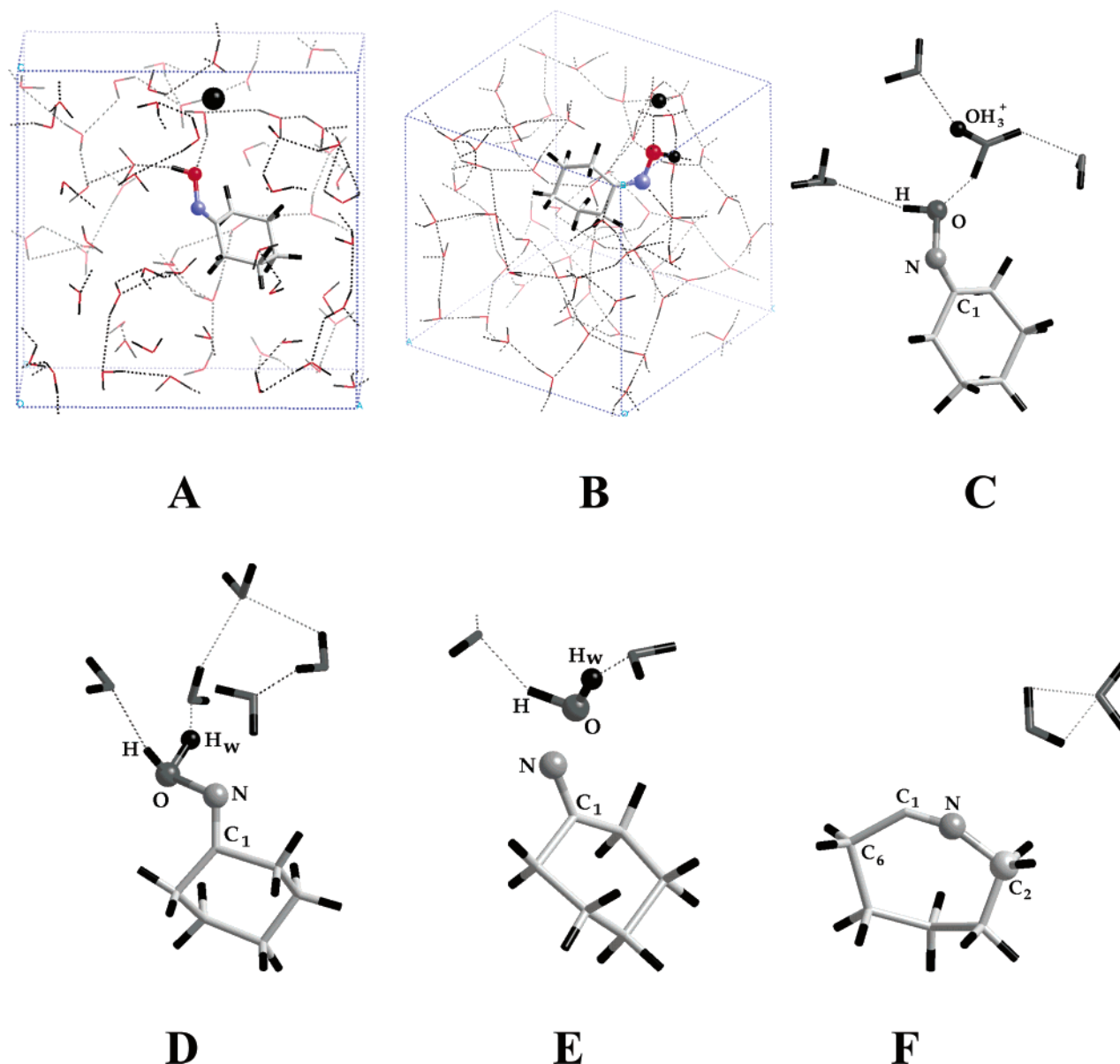


**Figure 3.** Simulated cyclohexanone oxime in supercritical water (A) and in normal liquid water (B). The solute is shown by thicker sticks, with N and C<sub>1</sub> evidenced as blue and red balls, respectively. Water molecules are the thinner v-shaped sticks, the excess proton is the big black ball, and H-bonds are shown as dashed lines. The main steps of the proton attack on the cyclohexanone oxime are the approach of H<sup>+</sup> (C), the attack on the O atom of the solute (D), the formation and release of a water molecule (E) and the seven-membered ring structure (F). The main atoms are labeled and shown as balls.

from one *sub-network* to another. In most of the configurations observed, when a look-alike Eigen complex could be identified, it was lacking at least one H<sub>2</sub>O monomer around OH<sub>3</sub><sup>+</sup>. As a consequence, the complex is an *unstable* H<sub>7</sub>O<sub>3</sub><sup>+</sup> structure (Figure 1C). Very rapidly, a proton of the OH<sub>3</sub><sup>+</sup>, different from the original incoming one, jumps on the nearest H-bonded H<sub>2</sub>O molecule. Hence, the excess proton can explore the local *sub-network* in a noticeably faster way than at ordinary liquid conditions, thus enhancing the efficiency of the reaction.<sup>41</sup>

The structure formed after the release of the H<sub>2</sub>O molecule is unstable: the carbon atom labeled C<sub>1</sub> in Figure 3E is in an sp<sup>2</sup> configuration and forms a double bond C<sub>1</sub>=N, leaving N in a nitrenium ion configuration, which turns out to be pretty unstable. In fact in about 50 fs the C<sub>1</sub>–C<sub>2</sub> bond weakens as a

result of the electron withdrawing by N<sup>+</sup>, and the ring opens following a Wagner–Meerwein shift mechanism, spontaneously stabilizing in a seven-membered ring configuration (Figure 3F) that can be seen as a precursor state of the  $\epsilon$ -caprolactam. This whole process occurs in a barrierless way and corresponds to an overall energy gain of  $\Delta F = 9.2$  kcal/mol and  $\Delta E = 10.5$  kcal/mol for the free and total energy, respectively, as checked by repeating the simulation within the metadynamics approach, by selecting as a collective variable the coordination number of N with C. Here and in the following we adopt the definition of coordination number of a species A with a species B,  $N_{\text{coord}}(A-B)$ , as in ref 30

$$N_{\text{coord}}(A-B) = \frac{1}{N_A} \sum_{A'=1}^{N_A} \sum_{B'=1}^{N_B} \frac{1 - (r_{A'B'}/d_{AB})^6}{1 - (r_{IJ}/d_{AB})^{12}} \quad (2)$$

(41) At the SCW conditions used in these simulations, the density is still sufficiently high to ensure a good H-bond connectivity. See, e.g.: Laria, D.; Marti, J.; Guàrdia, E. *J. Am. Chem. Soc.* **2004**, *126*, 2125.



where  $N_A$  and  $N_B$  are the number of atoms of species  $A$  and  $B$ , respectively,  $r_{IJ}$  is the interatomic distance, and  $d_{AB}$  is the typical equilibrium distance or chemical bond between  $A$  and  $B$ .

**3.2.2. Normal Liquid and Superheated Water.** Analogous free CPMD simulations of this same system with an excess proton were performed at two other thermodynamic conditions, corresponding to the ordinary liquid state ( $T = 300$  K,  $\rho = 1.00$  g/cm<sup>3</sup>) and to superheated water ( $T = 673$  K,  $\rho = 1.00$  g/cm<sup>3</sup>). In both cases, contrary to SCW, no density fluctuations are present, and the continuous H-bond network is such that both the O and the N atoms of the cyclohexanone oxime are *wet*. In the ordinary liquid state, the  $H^+$  propagates in the solvent and wanders for a long time ( $>5$  ps) before interacting with the solute. Indeed, the computed proton jump time for this system ( $\tau = 0.741 \pm 0.078$  ps) is roughly 1 order of magnitude greater than  $\tau_{SCW}$ , and the  $H^+$  moves around forming either Eigen or Zundel complexes, in agreement with the literature.<sup>39,40</sup> The greater stability of the Eigen  $H_9O_4^+$  complex with respect to SCW accounts for the longer  $\tau$ , and the reaction is slowed considerably with respect to SCW. If the  $H^+$  is in the vicinity of the O atom of the solute, then an  $H_2O$  molecule can be formed in the same way observed in SCW. Yet the presence of a solvation shell around the *wet* N atom prevents the spontaneous N—C<sub>2</sub> bond formation noticed in SCW, indicating that an activation barrier arises, separating the six-membered structure from the seven-membered ring.

A similar scenario holds also in the case of superheated water, where the only difference is the higher temperature. The molecular motion becomes faster, but the global features of the H-bond network do not change significantly with respect to the case of ordinary liquid water. This is reflected also in the pair correlation functions and integrated coordination numbers (Figure 2A (b) and B (b)) which, albeit slightly broader due to the increased entropy, still present features similar to ordinary liquid conditions. The excess proton can travel faster along the undisrupted H-bond network as a consequence of the increased temperature. However, the proton jump time, as computed from the simulation, decreases only to  $0.623 \pm 0.090$  ps, thus not as dramatically as in the SCW system. The diffusion mechanism can still be seen as a fluctuation between the Eigen complex and the Zundel shared proton, since a continuous H-bond network exists. The shorter lifetime of  $OH_3^+$  as an Eigen cation is due to a faster H-bond switch mechanism, induced by the high temperature. Its interaction with the solute molecule occurs within a simulation time of about 3.6 ps. However, in both the high-density cases, two reaction channels are possible: either the  $H^+$  attacks the OH group of the cyclohexanone oxime, or it interacts with the N atom and forms a stable N—H bond. Clearly, a higher solvent density has the effect of wetting both N and O (Figure 2), thus making possible the alternative reaction path of Figure 1A and jeopardizing the selectivity. This result is in agreement with the experimental observation about the presence of byproducts in superheated water.<sup>6–10</sup>

**3.2.3. Selectivity and Efficiency of the Reaction: Summary.** The following general picture may be drawn: in high-density water, both at high and low temperature, due to the continuous H-bond network, an excess proton is, on average, rather stabilized as an Eigen/Zundel complex in the solvent. Its transfer to the solute thus becomes slower, and due to the wetting of all the hydrophilic parts of the solute, no intrinsic selectivity

is present. On the contrary, at lower densities the H-bond network is disrupted, a lower stabilization of the proton occurs, and the  $H^+$  can selectively attack the hydrophilic parts of the solute due to their different wetting. This can offer a general clue to interpreting for example the experimental data of Figure 7 in ref 8, where an enhancement of the selective reaction rate is observed at decreasing H-bond ratio. The high temperature is in practice responsible only for the faster thermal motion, while the breaking down of the H-bond network and the drying of the N atom turn out to be the crucial factors in sending the reaction toward the desired pathway. As a matter of fact, density dependencies of the reaction rates in SCW are not unexpected<sup>42–44</sup> but very difficult to predict, since density changes can lead to either an increase<sup>45,46</sup> or a decrease<sup>47,48</sup> of the reaction rate. We can infer that this is dependent on the compound considered and its related solvation properties. Furthermore, in acid-catalyzed reactions, such as the Beckmann case considered here, the role of protons is essential. A simulation in the absence of excess  $H^+$  has shown that the approach of a water molecule to the —N—O—H group of the cyclohexanone oxime can still lead to the formation of the seven-membered ring structure. However, two drawbacks arise. First, a rather large energy barrier ( $\Delta E = 28.6$  kcal/mol,  $\Delta F = 26.5$  kcal/mol for the total and free energies, respectively) has to be overcome; in fact constrained dynamics<sup>29</sup> and metadynamics<sup>30,31</sup> simulations were needed to see the reaction occurring<sup>49</sup> and to estimate the activation energy (Figure 4A). Second, an alternative reaction path exists in which the approach of  $H_2O$  molecules has the simple effect of promoting a proton exchange between the —N—O—H group of the solute and a hydrogen of the incoming  $H_2O$  monomer, leaving the cyclohexanone oxime chemically unchanged and not resulting in any seven-membered ring structure formation. In the simple case of one water molecule (Figure 4B), this  $H^+$  exchange is characterized by an activation barrier of  $\sim 20.0$  kcal/mol, and this value is known to be even lower when two  $H_2O$  monomers participate, giving rise to a proton wire mechanism,<sup>11</sup> thus representing a strongly competing reaction channel.

**3.3. Second Step: Dissociation of  $H_2O$  and Formation of the Intermediate.** The seven-membered ring intermediate (Figure 3F) carries a positive charge that is localized mostly on the carbon atom  $C_1$ .<sup>50</sup> A water molecule in the vicinity, with the O atom pointing toward the carbon site  $C_1$  (Figure 5A), experiences a strong Coulombic attraction, leading to the dissociation of  $H_2O$  (Figure 5B). This occurs by overcoming a

(42) Chialvo, A.; Cummings, P. T. *J. Phys. Chem.* **1996**, *100*, 1309.

(43) Savage, P. E. *Chem. Rev.* **1999**, *99*, 603.

(44) Akiya, N.; Savage, P. E. *J. Phys. Chem. A* **2000**, *104*, 4433.

(45) Koo, M.; Lee, W. K.; Lee, C. H. *Chem. Eng. Sci.* **1997**, *52*, 1201.

(46) Holgate, H. R.; Tester, J. W. *J. Phys. Chem.* **1994**, *98*, 800.

(47) Oshima, Y.; Hori, K.; Toda, M.; Chommanad, T.; Koda, S. *J. Supercrit. Fluids* **1998**, *13*, 241.

(48) Steeper, R. R.; Rice, S. F.; Kennedy, I. M.; Aiken, J. D. *J. Phys. Chem.* **1996**, *100*, 184.

(49) In the cases discussed here, the activation barriers estimated via the Blue Moon approach turned out to be systematically higher than the corresponding metadynamics barriers by 1.2–0.6 kcal/mol. Of course, since the accuracy of first-principles approaches is at best within 1–2 kcal/mol, these differences are on the verge of the allowed precision. However, the fact that the slight overestimation is systematic seems to be due to the insufficiency of a single reaction coordinate in controlling all the *slow* degrees of freedom involved in the reaction.

(50) The atom labeled  $C_1$  is the only carbon site of the seven-membered ring to have a positive Mulliken (+0.28e) charge. All the other C sites along the ring are negative, while N is practically neutral, having a Mulliken charge of  $-0.08e$ . This indicates that, in the formation of the triple bond N—C<sub>1</sub>, the initially positive nitrogen (Figure 3E) withdraws electrons from  $C_1$  and the positive charge is transferred from N<sup>+</sup> to  $C_1^+$  (Figure 3F).

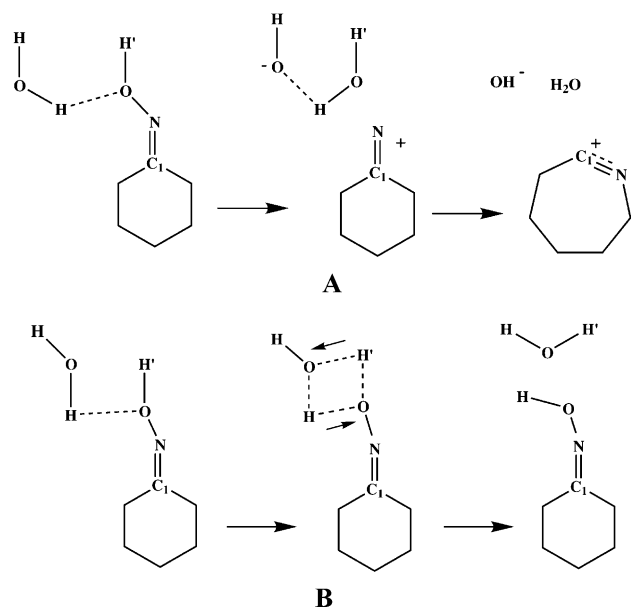


**Figure 4.** Two possible reaction paths, in the absence of protons, promoted by the attack of a water molecule on the O atom of the solute. (A) Formation of  $\epsilon$ -caprolactam with a large barrier. (B) Proton exchange with the solvent. The H atom belonging to the reactant (cyclohexanone oxime) has been labeled as H' for the sake of clarity. Details are given in the text.

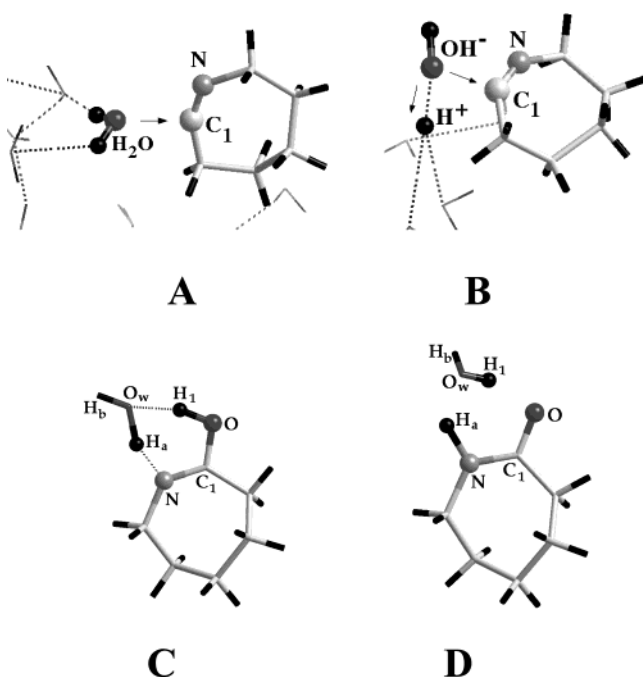


**Figure 5.** Final steps of the reaction. Approach of a water molecule to the positively charged carbon  $C_1$  of the seven-membered ring (A), dissociation of the  $H_2O$  leading to the intermediate structure (B), proton exchange between solvent and intermediate structure (C), leading to the formation of  $\epsilon$ -caprolactam (D). In the last two panels the H atom originally belonging to the solute is labeled  $H_1$ , while  $H_a$  and  $H_b$  refer to the hydrogen atoms of the approaching  $H_2O$  monomer. Other surrounding water molecules are shown as thin sticks and H-bonds as dashed lines.

rather modest activation barrier,  $\Delta E = 5.9$  kcal/mol and  $\Delta F = 5.2$  kcal/mol for the total and free energies respectively, as computed from the free energy metadynamics<sup>30,31</sup> approach. In the metadynamics simulations, the collective variables  $s_\alpha(t)$  were chosen to be the coordination number between  $C_1$  and the O of the closer  $H_2O$  molecule and the coordination number of the O of this water monomer with its bound H atoms.

These  $s_\alpha(t)$  variables account for the  $C_1$ –O bond formation and the  $H_2O$  dissociation, respectively. Fictitious effective masses  $M_\alpha = 40$  au and harmonic coupling constants  $k_\alpha = 0.6$  were used, and a new Gaussian contribution was added to the potential  $V(s,t)$  every 0.012 ps. A total simulation (meta)time of  $\sim 8$  ps was required to explore efficiently the free energy surface. We remark that this barrier is rather low if compared to the energy required for the self-dissociation of water.<sup>51</sup> This lowering is due to the Coulombic attraction between the positively charged  $C_1$  carbon and the lone pairs of the oxygen atom of the approaching water monomer. This result was basically confirmed by simulations performed within both the Blue Moon ensemble theory,<sup>29,49</sup> where the selected reaction coordinate was the distance  $\xi_1 = |\mathbf{R}(\text{O}) - \mathbf{R}(C_1)|$ , O being the oxygen atom of the closest water molecule, and  $C_1$ , the carbon atom labeled as in Figure 5.

Since the  $K_w$  of SCW at the thermodynamics conditions considered here is enhanced by about 3 orders of magnitude<sup>37</sup> with respect to the ordinary liquid conditions, not only protons but also their counterparts, hydroxyl anions  $OH^-$  originating from  $H_2O$  dissociation, might play some role, although this is expected to be a minor contribution. If an  $OH^-$  comes in the vicinity of the seven-membered ring structure, it experiences a Coulombic interaction that, again in a barrierless way, leads to the formation of the intermediate structure of Figure 5C, with a total energy gain of 21.2 kcal/mol. However, we stress that this result is just an insight into the effect of an  $OH^-$  originating the higher water dissociation rate in SCW with respect to ordinary liquid conditions and should not be understood as an increased basic character of the solvent.

### 3.4. Third (Final) Step: Proton Exchange with the Solvent.

This molecular structure closely resembles the  $\epsilon$ -caprolactam (Figure 1A), yet it is not the final product but an intermediate configuration requiring one more step to complete the reaction: the hydrogen labeled  $H_1$  (Figure 5C) has to be removed, while the nitrogen atom has to form a chemical bond with a nearby H.

A priori two scenarios are possible: either the  $H_1$  atom of the  $C_1$ –O– $H_1$  group is directly transferred to the N atom, or a water molecule comes into play and mediates the reaction via a proton exchange mechanism. In this case at least one water molecule, upon dissociation into  $OH^-$  and  $H^+$ , donates a proton to the nitrogen and grabs the H of the  $C_1$ –O– $H_1$  group, reverting to an  $H_2O$  molecule. Of course, more water molecules can be involved, leading to a proton wire mechanism.<sup>11</sup> However, our aim here is to inspect whether the proton transfer is mediated by the solvent. To achieve this, we performed both Blue Moon<sup>29</sup> and metadynamics<sup>30,31</sup> simulations.

In the case of the Blue Moon approach the distances  $\xi_2 = |\mathbf{R}(H_1) - \mathbf{R}(N)|$  and  $\xi_3 = |\mathbf{R}(H_a) - \mathbf{R}(N)|$  were the reaction coordinates selected for the direct proton transfer and the proton exchange with water, respectively, where the labels refer to Figure 5. In the metadynamics approach, instead, the two collective variables  $s_1$  and  $s_2$  selected are the coordination numbers of N with  $H_a$  and of  $O_w$  with  $H_1$ , the labeling being the same as in Figure 5. The fictitious masses and coupling constants are 35 au and 0.8 respectively for the two variables. A new Gaussian contribution is added to the potential  $V(s,t)$

(51) Sprik, M. *Chem. Phys.* **2000**, 258, 139.

every 0.012 ps and a total simulation (meta)time of  $\sim 8$  ps ensured an efficient exploration of the free energy surface.

As expected, both the approaches have shown that the proton exchange mechanism between the solvent and the solute (Figure 5) is the one characterized by the lowest activation barrier ( $\Delta F = 9.2$  and  $8.6$  kcal/mol from Blue Moon and metadynamics estimations, respectively). Direct transfer of the proton from the  $C_1-O-H_1$  to the N site of the solute would result in an energy barrier at least 2 times larger ( $20.5$  kcal/mol), and so is very unlikely.

In the water-mediated reaction path, a  $H_2O$  molecule approaches the intermediate structure (Figure 5C), forming H-bonds, and while donating one of its protons to the solute, it promotes the abstraction of the proton of the  $C_1-O-H_1$  group. The newly formed  $\epsilon$ -caprolactam (Figure 5D) turns out to be more stable by  $\Delta F = 6.7$  kcal/mol and  $\Delta E = 8.9$  kcal/mol with respect to the intermediate structure. This underscores again the essential and active role of the solvent at each stage of the reaction. We remark that the reaction path described here, involving interactions with  $H^+$  and  $OH^-$  and water molecules, is the one characterized by the most favorable pathway, requiring the overcoming of a modest energy barrier only in the final proton exchange stage. Simulations performed in the absence of protons and involving the dissociation of a single  $H_2O$  molecule donating simultaneously a proton to the N atom and an O to the  $C_1$  carbon resulted in energetically more demanding pathways, with activation barriers ranging from 14 to more than 20 kcal/mol.

#### 4. Concluding Remarks

The Beckmann rearrangement of cyclohexanone oxime into  $\epsilon$ -caprolactam promoted by SCW has been studied for the first time within a first-principles dynamical approach. The simulations have shown that the reaction, in its initial stage, is triggered mostly by the reduced density and the related fluctuations peculiar to the supercritical state. This can offer a clue to understanding the experimental results reported in for example ref 8; there it was observed that the rate constant increases remarkably, between 650 and 680 K, when the extent of H-bonds is reduced. Another important ingredient is the destabilization of the Eigen/Zundel complexes induced by the disrupted H-bond network. Furthermore, we have shown how water molecules cooperate in the final stages of the reaction. The general message of the present work is that SCW plays a fundamental role both in differentiating the solvation of the hydrophilic parts of the solute and in substituting an acid catalyst in the proton attack phase, thus offering a key to designing SCW triggered reactions.

**Acknowledgment.** We are grateful to Yutaka Ikushima, Michiel Sprik, Alessandro Laio, Marcella Iannuzzi, and Atsushi Oshiyama for fruitful discussions and valuable suggestions. Calculations were performed on the computer facilities at TACC, ISSP, and Tsukuba University.

JA049363F